Herpetologica, 78(1), 2022, 30–39

A New Bent-Toed Gecko of the *Cyrtodactylus marmoratus* Group (Reptilia: Gekkonidae) from Obi Island, Indonesia

Awal Riyanto[1,4,8], Fata H. Faz[2], A.A. Thasun Amarasinghe[3,4,8], Misbahul Munir[5], Yuli S. Fitriana[1], Amir Hamidy[1], Mirza D. Kusrini[2], and Paul M. Oliver[6,7]

[1] Museum Zoologicum Bogoriense (MZB), Research Center for Biology, National Research and Innovation Agency (BRIN), Jl. Raya Jakarta Bogor Km. 46 Cibinong, 16911 Jawa Barat, Indonesia
[2] Faculty of Forestry, Bogor Agricultural University, Darmaga Campus, West Java, Indonesia
[3] Department of Biology, Faculty of Mathematics and Natural Sciences, Universitas Indonesia, Kampus UI, 16424 Depok, Indonesia
[4] Association of Asian Herpetology (Asosiasi Herpetologi Asia), Jl. BSD Bintaro No. 88, Pondok Aren, 15228 Tangerang Selatan, Indonesia
[5] Graduate School of Global Environmental Studies, Kyoto University, Yoshida Nihonmatsu-cho, Sakyo-ku, 606-8501 Kyoto, Japan
[6] Queensland Museum, Department of Biological and Geological Sciences, South Brisbane, Australia
[7] Griffith University, Centre for Planetary Health and Food Security, Nathan, Queensland, Australia

Abstract: Based on phylogenetic and morphological evidence, we describe a new species of *Cyrtodactylus* from Obi Island in the northern Moluccas, Indonesia. The new species is genetically and morphologically allied to the Melanesian species *Cyrtodactylus papuensis* but is distinguished by its larger body size, fewer midbody scale rows, deep precloacal groove in males, and enlarged nonpored femoral scales and pored precloacal scales arranged in a continuous series. The new species is also genetically divergent from *C. papuensis* (*p*-distances of 19.0%–20.1% in the mitochondrial NADH dehydrogenase subunit 2 gene). Four species of *Cyrtodactylus* are now known from the northern Moluccas, but it is likely additional species remain unrecognized.

Key words: Maluku; Melanesia; New Guinea; Obi Island; Taxonomy; Wallacea; Weber's Line

The Moluccas are a group of islands in Indonesia in the eastern portion of Wallacea that are just to the west of Lydekker's Line (van Welzen et al. 2011). The northern half of the Moluccas is dominated by the following four relatively large islands: Halmahera, Ceram, Buru, and Obi. These islands show high levels of endemism of birds (Gill and Donsker 2012); however, their herpetofauna is poorly documented, with a single targeted survey by Edgar and Lilley (1993). *Cyrtodactylus* is an exceptionally diverse clade of geckos with over 300 described species (Uetz and Hallermann 2021) that has radiated on landmasses to both sides of Wallacea (e.g., New Guinea and Borneo). At present, only the following three species of *Cyrtodactylus* are recognized from the northern Moluccas: *C. deveti* (Brongersma 1948), *C. halmahericus* (Mertens 1929), and *C. nuaulu* Oliver, Edgar, Mumpuni et al. 2009. *Cyrtodactylus papuensis* (Brongersma 1934) has also been recorded from Aru Islands in the southern Moluccas (P.M. Oliver, personal observation), and an additional, probable undescribed, taxa in the *C. darmandvillei* group occurs on the Kai Islands (Karin et al. 2018; Oliver et al. 2018). Here, we present genetic and morphological data that indicate a series of six *Cyrtodactylus* specimens from Obi Island represent an additional and previously unrecognized species. Genetic data place these specimens in the *C. marmoratus* group (sensu Grismer et al. 2021), filling a gap in the wide distribution of this group across Sumatra, through Java, and east into New Guinea.

Materials and Methods

In December 2016 and January 2018, one of us (F.H. Faz) visited Obi Island (Fig. 1) in Central Maluku Province, Indonesia, and collected a series of six *Cyrtodactylus* specimens. Specimens were collected by hand, euthanized with sodium pentobarbital, and fixed in 10% buffered formalin prior to storage in 70% ethanol. We preserved liver tissue samples for DNA analysis in 95% ethanol. Latitude, longitude, and elevation of localities of specimens collected were recorded using a Garmin GPSmap 60CSx using WGS84 map datum. All specimens are permanently deposited at the Museum Zoologicum Bogorienese (MZB), Cibinong, West Java, Indonesia. Additional comparative material examined for morphological comparisons is listed in the Appendix.

Although samples of the *C. marmoratus* group from New Guinea have on occasion been referred to as *C. marmoratus* Gray 1831, it has been shown on several occasions that these populations are *C. papuensis* (see Rösler et al. 2007; Tallowin et al. 2018). Accordingly, in this paper, we restrict *C. marmoratus* to Java.

New sequences generated in this work were deposited in GenBank, and additional genetic data were downloaded from GenBank (Table 1). As noted above and following Riyanto et al. (2020), we consider DNA sequences from specimens from Cibodas, West Java to represent true *C. marmoratus*. Following Grismer et al. (2021), *Hemidactylus frenatus* was used as an outgroup. We extracted genomic DNA from liver samples by using a phenol–chloroform protocol (Sambrook et al. 1989). A partial mitochondrial sequence of the protein-encoding gene NADH dehydrogenase subunit 2 (ND2) was amplified with the primers M112F (5′-AAGCTTTCGGGGCCCATACC-3′) and M1123R (5′-GCTTAATTAAAGTGTYTGAGTTGC-3′; Oliver et al. 2016). The PCRs were performed in 25-μL total volumes using Top Taq™ by Qiagen comprising 1.0 μL DNA template, 2.5 μL 10× Top Taq PCR buffer™, 0.5 μL 10 mM dNTP mix, 2.5 μL 10× CoralLoad, 5 μL 5× Q solution, 1.0

[8] Correspondence: e-mail, awal_lizards@yahoo.com, thasun.amarasinghe@ui.ac.id

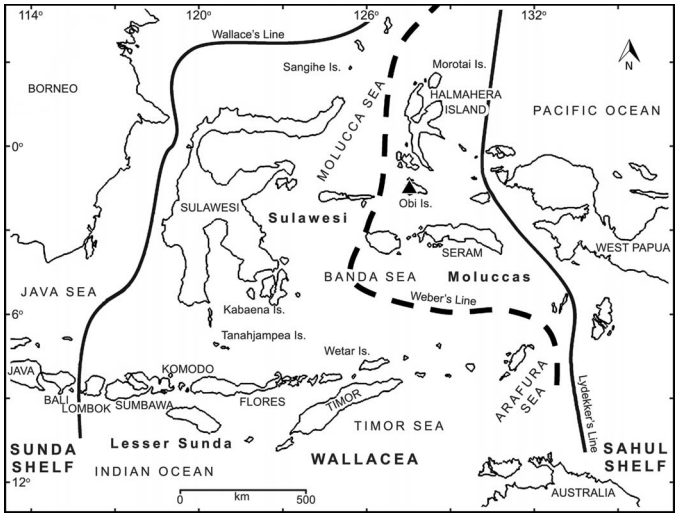

FIG. 1.—The distribution map for *Cyrtodactylus papeda* sp. nov. (triangle) with the biogeographic boundaries of Wallacea.

μL light strand primer, 1.0 μL heavy strand primer, 0.125 μL Top Taq DNA polymerase with appropriate buffer, and ddH_2O to volume. PCRs were executed on an Eppendorf Mastercycler instrument under the following conditions: an initial denaturing step at 94°C for 9 min, a second denaturing step at 94°C for 45 s, annealing at 60°C for 45 s, and a cycle extension at 72°C for 1 min, for 35 cycles. Purified PCR products were sequenced by 1st Base Asia, Singapore. We assembled and aligned DNA sequences with available data from GenBank data (Table 1) using Clustal W in MEGA X v10.1.7 (Kumar et al. 2018). The uncorrected *p*-distance (sequence divergence) was calculated in MEGA X, and all ambiguous positions were removed for each sequence pair (pairwise deletion option).

We estimated phylogenetic relationships by using a final alignment of 1041 base pairs (bp) of the ND2 gene and its flanking tRNAs using maximum likelihood (ML) and Bayesian inference. ML analysis was run on the IQ-TREE (Nguyen et al. 2015). We used the function -m MFP+MERGE (Lanfear et al. 2012) to identify the partitioning strategy and molecular models (first codon TPM2u+F+G4: second codon HKY+F+G4: third codon TPM3u+F+R2). We ran 5000 bootstrap replicates by using the ultrafast bootstrap method (Hoang et al. 2017). Nodes with bootstrap values above 95% were considered highly supported (Minh et al. 2013). We conducted our Bayesian inference analysis using MrBayess v3.2.6 (Ronquist and Huelsenbeck 2003) under GTR+Gamma as the best-fitting model, for 10 million generations with parameter and topology sampling every 1000 generations and Markov Chain Monte Carlo diagnosis frequency of 100,000, and later discarded 25% of the first analysis as burn-in.

For morphological analyses, we made comparisons with specimens (Appendix) and published descriptions of *Cyrtodactylus* from Melanesia, the Moluccas, and elsewhere in Southeast Asia. All specimens examined are held at the MZB. We scored specimens for morphological and morphometric characters used in recent descriptions of the genus *Cyrtodactylus* (e.g., Oliver et al. 2009; Riyanto et al. 2018a,b; Amarasinghe et al. 2020). Measurements were taken with Mitutoyo digital calipers to the nearest 0.1 mm under an AmScope SM-1BZ-RL dissecting microscope on the right side of the body. We took the following measurements: snout–vent length (SVL), from tip of snout to vent; tail length (TL), from vent to tip of tail; head length (HL), distance from tip of snout to posterior edge of retroarticular process of lower jaw; head width (HW), in a straight line at angle of

TABLE 1.—Species used in the molecular study with locality information and GenBank accession numbers. Museum acronyms follow Uetz et al. (2019); Is. = island, Gn. = mountain, FR = forest reserve, UFRR = Upper Fly River Region.

Species	Specimen voucher	Locality	GenBank accession no.	Reference
Cyrtodactylus papeda sp. nov.	MZB.Lace. 14052	Obi Is., Moluccas, Indonesia	OM158779	This study
C. batucolus	LSUHC 8933	Besar Is., Malaysia	JQ889178	Johnson et al. 2012
C. consobrinus	LSUHC 6586	Selangor, West Malaysia	JX440532	Wood et al. 2012
C. darmandvillei	WAMR 98497	East Nusa Tenggara, Indonesia	KU232616	Riyanto et al. 2015
C. darmandvillei	WAM R98393	Sumbawa Besar, Indonesia	JX440533	Wood et al. 2012
C. jellesmae	MVZ239337	Luwu Utara, South Sulawesi, Indonesia	JX440542	Wood et al. 2012
C. kimberleyensis	WAMR164144	Montalivey Is., Australia	JX440544	Riyanto et al. 2015
C. marmoratus	MZB.Lace. 13300	Cibodas, West Java, Indonesia	KR921721	Harvey et al. 2015
C. marmoratus	ABTC 48075	Cibodas, West Java, Indonesia	GQ257747	Wood et al. 2012
C. pantiensis	LSUHC 8906	Gn. Panti FR, Johor, West Malaysia	JQ889185	Johnson et al. 2012
C. cf. *papuensis*	JAM 2242	Buru Is., Indonesia	MF169967	Brennan et al. 2017
C. cf. *papuensis*	MZB.Lace. 5419	Raja Ampat, Papua Barat, Indonesia	JQ820315	Oliver et al. 2012
C. papuensis	SAMAR 62651	Libano, Papua New Guinea	JQ820321	Oliver et al. 2012
C. papuensis	SAMAR 62652	Libano, Papua New Guinea	JQ820320	Oliver et al. 2012
C. papuensis	PMO3	UFRR, Papua New Guinea	OM517150	Tallowin et al. 2018
C. papuensis	AA1914	Fakfak region, Indonesia	OM517149	Tallowin et al. 2018
C. petani	MZB.Lace. 15000	Klakah, East Java, Indonesia	MT704864	Riyanto et al. 2015
C. sadleiri	SAMAR 34810	Christmas Is., Australia	JQ820309	Riyanto et al. 2015
C. semenanjungensis	LSUHC 89000	Gn. Panti FR, Johor, West Malaysia	JQ889177	Johnson et al. 2012
C. semiadii	MZB.Lace. 14818	Tanjungsari, Yogyakarta, Indonesia	MT704866	Riyanto et al. 2020
C. seribuatensis	LSUHC 6348	Seribuat Is., Malaysia	JX440557	Wood et al. 2012
Cyrtodactylus sp.	CMD 384	East Timor	KU232622	Riyanto 2012
C. tiomanensis	LSUHC 6251	Tioman Is., Pahang, West Malaysia	JX440563	Wood et al. 2012
C. equestris	AMSR 135520	Sandaun, Papua New Guinea	KT835458	Oliver et al. 2016
C. rex	SAMAR 67637	Sandaun, Papua New Guinea	KT835460	Oliver et al. 2016
Hemidactylus frenatus	LSUHC 4871	Bukit Bakong, Pahang, Malaysia	GQ458049	Bauer et al. 2010

TABLE 2.—*p*-distances among taxa in the *Cyrtodactylus marmoratus* group based on the mitochondrial ND2 gene (590 bp).

No.	Species	1	2	3	4	5
1	*C. papeda* sp. nov.	—				
2	*C. marmoratus* (West Java, Indonesia)	22.2	—			
3	*C.* cf. *papuensis* (Buru Island, Indonesia)	17.2	21.1	—		
4	*C.* cf. *papuensis* (Raja Ampat, West Papua, Indonesia)	16.9	19.9	7.7	—	
5	*C. papuensis* (Fak-Fak, Indonesia; Libano and Fly River, Papua N-Guinea)	19.0–20.1	20.4–20.6	9.9–10.6	9.9–10.9	—
6	*C. semiadii*	22.0	20.2	18.7	18.3	19.5–21.1

jaws; head height (HH), maximum height of head between occiput and throat; snout length (SL), from tip of snout to anteriormost edge of orbit; eye to ear distance (EE), measured from edge of orbit to anterior edge of ear opening; ear length (EL), maximum length of ear opening; orbit diameter (OD), horizontal diameter of orbit; rostral height (RH), maximum height of rostral shield; rostral width (RW), distance between border of rostral shield and first supralabial scales on right and left sides; mental length (MEL), maximum length of mental shield; mental width (MEW), maximum width of mental shield; forearm length (FAL), taken on dorsal surface posterior margin of elbow while flexed at 90° to inflection of dorsally flexed wrist; axilla–groin length (AG), measured from axilla to groin; and tibia length (TBL), measured on ventral surface from posterior surface of knee while flexed at 90° to the base of the heel.

We counted supralabial scales (counted from the rostral scale to the largest scale immediately posterior to dorsal inflection of posterior portion of upper jaw), infralabial scales (number of labial scales of lower jaw, beginning with first scale bordering mental shield, ending with last enlarged scale bordering angle of jaw), dorsal tubercles (number of longitudinal tubercle rows on dorsum at midbody between ventrolateral folds), paravertebral tubercles (tubercles along paravertebral region, counted between postaxial margin of arm and preaxial margin of leg), ventral scales (number of ventral scales at midbody, counted in one row between ventrolateral folds across the belly), number of lamellae under fingers 1–5 ($F_{1–5}$; subdigital lamellae counted from point where interdigital skin contacts digit regardless of condition of scales under digit at this point, including fractured scales but not the elongate ungual scale at the base of the claw [claw sheath] or lamellae that extend onto the palm at base of digit), and number of lamellae under toes 1–5 ($T_{1–5}$; subdigital lamellae counted from point where interdigital skin contacts digit regardless of condition of scales under digit at this point, including fractured scales but not including the elongate ungual scale at the base of the claw or lamellae that extend onto plantar surface at the base of the digit). Basal subdigital scales were counted from the most proximal scale at least twice as large as adjacent palmar scales following Bauer et al. (2010). Where relevant, we also noted the following characters: presence of tubercles on the dorsal surfaces of the brachium (upper arm), antebrachium (forearm), and thigh; presence of enlarged precloacofemoral scales and the extent to which they formed a continuous series; and the presence of transversely enlarged median subcaudals. We follow Kathriner et al. (2014) and Mecke et al. (2016a,b) in describing the morphology of precloacal depressions. Sex was determined as male (1) if preserved specimens showed enlarged hemipenial pockets and/or (2) by viewing the hemipenes via a small lateral incision made at the base of the tail. To examine smaller characters such as keeling in the ventrals, following Amarasinghe et al. (2015) and Harvey et al. (2015), we applied the reversible stain methylene blue in 70% ethanol. Color notes were taken from digital images of living specimens prior to preservation.

To assess the morphometric variation between the new species and its closest congener *C. papuensis*, we performed a separate Kruskal–Wallis one-way analysis of variance test because of the small sample size (Zar 2010). Statistically informative tests could not be performed on separate sexes because of small sample sizes. Therefore, only 15 adult specimens (9 specimens of *C. papuensis* and 6 specimens [all types] of the new species) were used for the statistical analysis. Juveniles were excluded to avoid the bias of allometry in the statistical analysis. Univariate and multivariate analyses were conducted on 10 morphometric ratios (AG/SVL, HL/SVL, FAL/SVL, TBL/SVL, HW/HL, OD/HL, OD/SL, SL/HL, EE/HL, and EE/OD). Each morphometric ratio was treated as the dependent variable and the population as the predictor variable. A multivariate analysis was conducted using Principal Component Analysis (PCA) to reduce the highly correlated multidimensional data matrix into a few uncorrelated variables (i.e., principal components [PCs]). We used the princomp function in the R statistical software program (v4.0.4.; R Core Team 2021) based on a correlation matrix of 10 morphometric ratios. A biplot of the first two PC scores was used to examine the morphometric differentiation between the populations. All statistical analyses were conducted using the R statistical software program (v4.0.4.; R Core Team 2021).

RESULTS

Molecular analyses indicated that the *Cyrtodactylus* sample from Obi Island is nested within the *C. marmoratus* group (sensu Grismer et al. 2021). The broader *C. marmoratus* group received moderate support (ultrafast bootstrap, >77; Bayesian posterior probabilities, >0.93). In addition to species and candidate species listed in Grismer et al. (2021), we found the *C. marmoratus* group also included *Cyrtodactylus semiadii* from Java. The Javan taxa in the *C. marmoratus* group are all deeply divergent from their sampled relatives from the Moluccas (Obi, Buru) and Melanesia (Table 2; Fig. 2). The population from Obi Island is most closely related to a suite of samples assigned to *C. papuensis* from across Buru, the Raja Ampat Islands, and southern New Guinea. However, it differs from these samples by a minimum *p*-distance of 16.9% (Table 2).

Three out of 10 morphometric ratio mean comparisons also showed significant differences between the population in Obi Island and *C. papuensis*, namely, OD/HL ($\chi^2 = 8.0$, $P < 0.001$), EE/OD ($\chi^2 = 8.7$, $P < 0.001$), and OD/SL ($\chi^2 = 5.0$, $P = 0.02$), indicating the population in Obi Island has a

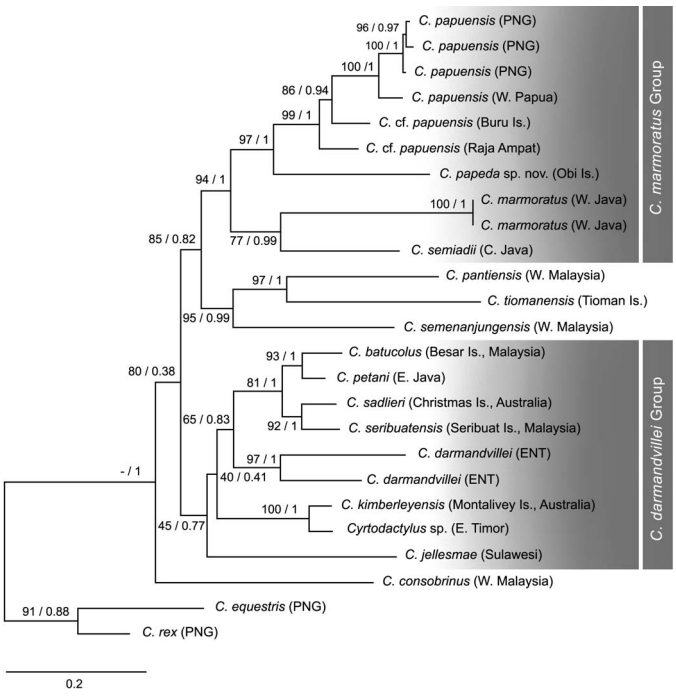

FIG. 2.—Fifty percent majority-rule consensus phylogram from Bayesian inference of the mitochondrial ND2 region of members of *Cyrtodactylus marmoratus* and groups. Numbers above or below branches indicate the values of Ultrafast Bootstrap (UFBoot) based on a separate maximum likelihood (ML) followed by values from Bayesian posterior probabilities (BPPs); W = west, C = central, E = east, PNG = Papua New Guinea, ENT = East Nusa Tenggara, Is. = island); outgroup taxon, *Hemidactylus frenatus* is not shown.

TABLE 3.—Principal component analysis (PCA) and loadings for *Cyrtodactylus papeda* sp. nov. and *C. papuensis*. Principal components (PCs) 1 and 2 collectively explained 52.5% of variation. SVL = snout–vent length; AG = axilla–groin length; HL = head length; HW = head width; OD = orbit diameter; SL = snout length; EE = eye to ear distance; FAL = forearm length; TBL = tibia length.

PCA variable	PC 1	PC 2	PC 3	PC 4	PC 5	PC 6
Standard deviation	1.7230	1.5110	1.3017	1.0650	0.97716	0.72149
Proportion of variance	0.2970	0.2283	0.1694	0.1134	0.09548	0.05206
Cumulative percentage	29.7	52.5	69.5	80.8	90.4	95.6
Loadings						
AG/SVL	−0.1229	−0.1028	0.1734	0.7162	0.4483	−0.4086
HL/SVL	0.0580	0.4877	−0.3216	0.0568	−0.2364	−0.6157
FAL/SVL	−0.1535	−0.0034	−0.4878	−0.0315	0.6722	0.2244
TBL/SVL	−0.3870	−0.1741	−0.0323	−0.4977	0.1165	−0.5628
HW/HL	−0.1085	−0.5299	0.3480	−0.2360	0.0728	−0.1593
OD/HL	−0.4520	0.2504	0.3345	0.1073	−0.0988	0.1170
OD/SL	−0.3137	0.4289	0.3836	−0.1025	0.1399	0.1094
SL/HL	−0.2102	−0.4020	−0.1149	0.3899	−0.4524	0.0094
EE/HL	0.3832	0.1443	0.4729	0.0011	0.1392	−0.0921
EE/OD	0.5502	−0.1061	0.1026	−0.0734	0.1379	−0.1648

relatively larger eye (orbit) and shorter head, snout, and eye–ear lengths. A multivariate analysis by PCA also differentiated the population in Obi Island and the closely related *C. papuensis* (Fig. 3A). PC 1 and PC 2 collectively explained 52.5% of variation in the morphometric data matrix (Table 3; Fig. 3A). Morphometric ratios HL/SVL, EE/HL, and EE/OD loaded positively with PC 1. Additionally, morphometric ratios HL/SVL, OD/HL, OD/SL, and EE/HL loaded positively with PC 2 (Table 3). Overall, morphometric ratios

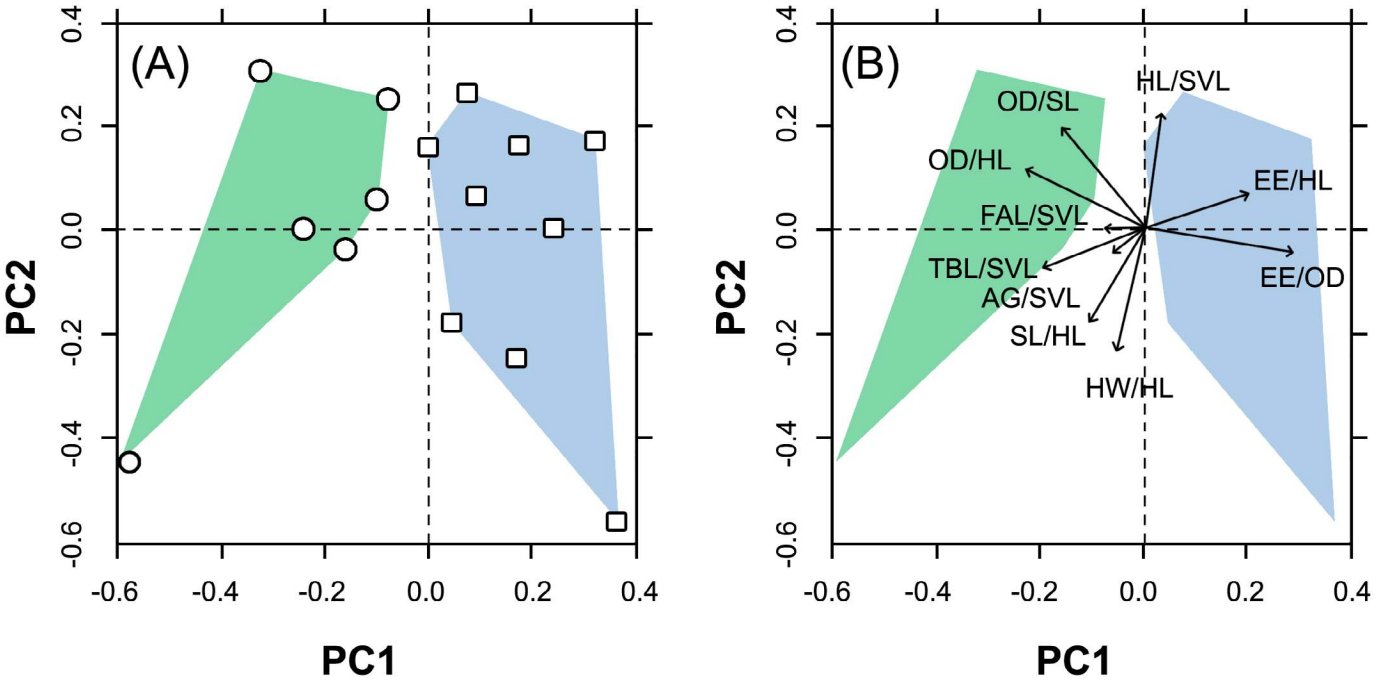

FIG. 3.—(A) Principal component analysis (PCA) biplot of morphometric variation between the population in Obi Island (circles) and its Melanesian congener *C. papuensis* from West Papua (squares) clearly shows the morphological distinctiveness of the new species. Each point represents an individual specimen, and the relative distance between two points is equivalent to amount of dissimilarity; (B) the same base biplot with vectors associated with population clusters. SVL = snout–vent length; AG = axilla–groin length; HL = head length; HW = head width; OD = orbit diameter; SL = snout length; EE = eye to ear distance; FAL = forearm length; TBL = tibia length; PC = principal component. A color version of this figure is available online.

TABLE 4.—Morphometric (in mm) and meristic characters of the holotype and paratypes of *Cyrtodactylus papeda* sp. nov. M = male; F= female; reg. = regenerated; — = not applicable.

	Cyrtodactylus papeda sp. nov.						
	Holotype	Paratypes (n = 6)					
Character	MZB.Lace. 14052	MZB.Lace. 14578	MZB.Lace. 14575	MZB.Lace. 14576	MZB.Lace. 14053	MZB.Lace. 14574	MZB.Lace. 14577
Sex	M	M	M	M	F	F	F
Snout–vent length	60.7	62.9	51.1	56.6	55.9	67.5	84
Tail length	63.2 reg.	69.1 reg.	69.1	64.9 reg.	67.5	82.7	69.1
Head length	17.5	18.1	14.9	15.6	16.4	18.9	18.7
Head width	10.2	11.2	9.3	10.4	9.8	11.5	9.8
Head height	6.6	7.0	5.7	6.7	6.6	7.5	7.3
Snout length	7.6	6.9	5.7	6.8	6.7	6.9	6.8
Eye–ear distance	4.5	4.4	4.2	3.2	4.8	5.6	5.7
Ear length	1.7	1.1	1.3	1.7	1.6	1.5	1.9
Orbit diameter	5.3	4.7	4.8	4.5	4.7	5.7	5.2
Rostral height	1.4	1.6	0.9	1.5	1.4	1.5	1.3
Rostral width	1.9	2.2	1.8	2.4	2.4	2.7	2.0
Mental length	1.3	2.2	1.4	1.4	1.7	1.3	2.0
Mental width	1.8	2.4	2.2	2.4	2.2	2.5	2.5
Forearm length	9.1	9.9	7.4	8.6	8.6	9.9	8.7
Axilla–groin length	28.6	25.5	21.2	25.9	27.5	32.2	31.4
Tibia length	10.7	12.2	10.1	11.5	10.3	11.7	11.0
Supralabials	13	13	12	10	13	12	13
Infralabials	9	10	10	9	10	10	9
Dorsal tubercle rows	17	17	15	17	14	17	14
Paravertebral tubercles	32	27	30	30	34	34	32
Ventral scale rows across belly	45	51	54	50	50	47	50
Precloacal pores	5	5	5	5	—	—	—
Lamellae under fingers 1–5	10-14-16-18-16	11-16-19-18-17	11-16-20-20-15	12-16-20-20-16	11-16-19-19-16	12-17-20-21-18	12-16-18-19-16
Lamellae under toes 1–5	12-16-20-21-21	12-18-21-22-19	10-17-23-23-20	12-16-21-23-19	12-17-20-22-20	13-18-23-23-20	13-17-20-22-19

HL/SVL and EE/HL were positively associated with the population of Obi Island, whereas EE/OD showed negative associations (Fig. 3B).

We present diagnostic morphological, morphometric, and meristic data taken for the type specimens in Table 4. Morphological analyses revealed a suite of characters to diagnose the population of Obi Island from all other known species of the genus *Cyrtodactylus* from Wallacea and Melanesia (Tables 5 and 6). Based on morphological and genetic differences, we describe the *Cyrtodactylus* population from Obi as a new species.

SYSTEMATICS

Cyrtodactylus ***papeda*** sp. nov.
(Tables 4–6; Figs. 1–5)

Holotype.—Adult male (MZB.Lace. 14052; Field Number: Obi-2-Hb), from Kawasi, Obi Island (1°32.047′S, 127°32.046′E, datum = WGS84; 70 m above sea level), Halmahera Selatan, Maluku Province, Indonesia, collected on 5 December 2016 by F.H. Faz.

Paratypes.—Adult females (MZB.Lace. 14053, 14574, 14577), subadult male (MZB.Lace. 14575), and adult males (MZB.Lace. 14576, 14578) collected on 6 January 2018; other collection details same as the holotype.

Diagnosis.—The following combination of characters distinguishes *C. papeda* sp. nov. from all other congeners: adult males reaching 62.9 mm SVL and females 84.0 mm SVL; dorsal tubercles present on brachium, antebrachium, and along the ventrolateral fold; 14–17 irregular dorsal tubercle rows at midbody; 27–34 paravertebral tubercles per series; 45–54 ventral scale rows across belly; deep precloacal groove with 5 pores in males; enlarged femoral and precloacal scales arranged in a continuous series; no femoral pores; 21–23 lamellae under fourth toes; and subequal median subcaudal scales not transversely enlarged.

Description of holotype.—A moderate-sized *Cyrtodactylus* species reaching 60.7 mm SVL; head triangular in dorsal view, distinct from neck; tubercles present on the occiput and dorsolateral of head; head long, HL 28.8% of SVL; head rather wide, HW 58.3% of HL; head wider than high, HW 63.5% of HH; snout tapering to relatively blunt tip in dorsal profile, relatively long, SL 148.4% of OD; loreal region weakly inflated, interorbital region and top of snout concave, canthus rostralis rounded; supraciliaries extending from anterior-ventral to posterior-dorsal edge of eye, longest at the anterior-dorsal part; ear opening small, dorsoventrally oblong, and oriented about 45 degrees to apex of rictus. Rostral rectangular, RH 71.8% of RW; bordered posterolaterally by first supralabials and naris, and dorsally by 4 postrostral scales; naris oval, bordered anteriorly by rostral, anterodorsally by 1 postrostral, posteriorly by 5 scales in right side and by 5 scales in left side, and ventrally by first supralabials; orbit separated from supralabials by 2 rows of small lorilabial scales; 13 supralabial scales to angle of jaw; 9 infralabial scales. Mental triangular, slightly wider than long, MEL 74.2% of MEW; bordered laterally by first infralabials, posteriorly by 1 pair of enlarged first postmentals, which contact medially over about 0.76 mm; second postmentals ovoid, about one-third of the first postmentals and separated from each another by 2–5 granular scales; gular sales small, granular, grading to slightly smaller size posteriorly.

Body elongate, AG 47.2% of SVL; dorsal scales small, granular, interspersed with large, conical, semiregularly arranged, keeled tubercles; ventrolateral body folds with blunt conical tubercles; 17 dorsal tubercle rows; 32 paraver-

TABLE 5.—Characters used to distinguish *Cyrtodactylus papeda* sp. nov. and congeners in Wallacea. — = not applicable; ? = unknown.

Species	Max. SVL (mm)	Tubercles on brachium	Ventral scale rows across belly	Median subcaudals (in original tail)	No. of subdigital lamellae under Toe IV	No. of precloacal pores	No. of femoral pores	No. of femoro-precloacal pores	Femoral scales (in case no pores)	Precloacal depression	Dorsal body coloration	Source
C. papeda sp. nov.	84	Present	45–54	Subequal	21–23	5	Absent	—	Enlarged	Groove	Blotched	This study
C. batik	113	Present	48–57	Enlarged	24–27	Absent	Absent	—	Subequal	Absent	Banded	This study
C. celatus	44	Absent	34–42	Subequal	15–18	4	Absent	—	Subequal	Groove	Blotched	Riyanto et al. (2016)
C. darmandvillei	82	Present	34–36	Enlarged	23–24	—	—	?	—	Absent	Blotched	Mecke et al. (2016a,b)
C. deveti	106	Absent	40–49	Enlarged	25–28	—	—	29–31	—	Absent	Banded	This study
C. fumosus	78	Absent	37–50	Subequal	17–23	10–11	3	—	—	Groove	Blotched	Mecke et al. (2016a,b)
C. gordongekkoi	73	Absent	30	Subequal	22–23	Absent	Absent	—	—	Absent	Blotched	Mecke et al. (2016a,b)
C. halmahericus	78	Present	39–42	Subequal	22	—	—	48–53	—	Groove	Blotched	This study
C. hitchi	79	Absent	39–45	Enlarged	18–21	Absent	Absent	—	Subequal	Absent	Banded	This study
C. jatnai	67	Present	40–48	Subequal	17–19	—	—	40–43	—	Absent	Blotched	Amarasinghe et al. (2020)
C. jellesmae	70	Absent	40–54	Subequal	16–23	Absent	Absent	—	Subequal	Absent	Blotched	This study
C. laevigatus	47	Absent	30–34	Subequal	10–15	Absent	Absent	—	Subequal	Absent	Mottled	Mecke et al. (2016a,b)
C. nuaulu	88	Present	48–55	Subequal	17–20	6	Absent	—	Subequal	Groove	Striped	Oliver et al. (2009)
C. spinosus	83	Present	38–44	Subequal	19–21	12–13	Absent	—	Subequal	Pit	Banded	Linkem et al. (2008)
C. tahuna	79	Present	49–50	Subequal	20–24	14	5	—	—	Pit	Blotched	Riyanto et al. (2018a)
C. tambora	47	Absent	40	Subequal	16–17	5–6	Absent	—	Enlarged	Groove	Blotched	Riyanto et al. (2017)
C. tanahjampea	76	Present	28–34	Subequal	18–23	—	—	20–24	—	Absent	Blotched	Riyanto et al. (2018b)
C. wallacei	114	Present	45–49	Enlarged	17–25	Absent	Absent	—	Subequal	Absent	Banded	Linkem et al. (2008)
C. wetariensis	67	Absent	36–38	Subequal	20–22	—	—	23–27	—	Absent	Blotched	Mecke et al. (2016a,b)

tebral tubercles in each row. Ventral scales larger than dorsal scales, smooth, flat, imbricate, 45 ventral scale rows between ventrolateral body folds across the belly; enlarged scales immediately anterior to the cloacal opening absent.

Forelimbs relatively short, FAL 15.0% of SVL; dorsal scales on forelimbs granular; dorsal surface of upper and lower arms, with few tubercles close to elbow and be multiply number near to the axilla; palmar scales flat,

TABLE 6.—Characters used to distinguish *Cyrtodactylus papeda* sp. nov. and congeners in Melanesia. — = not applicable; ? = unknown.

Species	Max. SVL (mm)	Tubercles on brachium	Ventral scale rows across belly	Median subcaudals (in original tail)	No. of subdigital lamellae under Toe IV	No. of precloacal pores	No. of femoral pores	No. of femoro-precloacal pores	Femoral scales (in case no pores)	Precloacal depression	Dorsal body coloration	Source
C. papeda sp. nov.	84	Present	45–54	Subequal	21–23	5	Absent	—	Enlarged	Groove	Blotched	This study
C. aaroni	83	Absent	33–40	Enlarged	21–25	5–8	5–10	—	—	Absent	Banded	Günther and Rösler (2003)
C. arcanus	92	?	37–40	Subequal	9–10	?	?	?	Enlarged	?	Banded	Oliver et al. (2012)
C. atremus	118	Present	40–47	Subequal	24–31	Absent	Absent	—	Enlarged	Absent	Banded	Kraus and Weijola (2019)
C. boreoclivus	109	Absent	36–44	Enlarged	11–13	12	17–25	—	—	Absent	Banded	Oliver et al. (2011)
C. capreoloides	84	Absent	31–39	Subequal	22–23	13–14	16–24	—	—	Pit	Banded	Rösler et al. (2007)
C. crustulus	102	Present	40–49	Subequal	9–12	Absent	Absent	—	?	Absent	Botched	Oliver et al. (2020)
C. derongo	112	?	46–48	Subequal	24–26	?	?	?	?	Absent	Blotched	Brown and Parker (1973)
C. epiroticus	134	Absent	31–45	Enlarged	23–29	—	—	60–82	—	Absent	Banded	Kraus (2008)
C. equestris	139	Present	39–59	Subequal	11–13	6–8	8–15	—	—	Absent	Banded	Oliver et al. (2016)
C. irianjayaensis	163	Absent	36–44	Subequal	28–35	—	—	9–17	—	Absent	Banded	Rösler et al. (2007)
C. klugei	143	Absent	43–49	Enlarged	27–31	—	—	66–76	—	Absent	Banded	Kraus (2008)
C. loriae	137	Absent	37–59	Subequal	20–29	—	—	30–81	—	Pit	Banded	Rösler et al. (2007)
C. louisiadensis	138	Absent	44–58	Enlarged	27–31	18–20	21–24	—	—	Absent	Banded	Rösler et al. (2007)
C. manos	75	Absent	46	Subequal	11	?	?	—	?	?	Banded	Oliver et al. (2019)
C. medioclivus	103	Absent	43	Enlarged	9–14	12–13	19–24	—	—	Absent	Banded	Oliver et al. (2012)
C. mimikanus	90	Present	34–48	Enlarged	?	7–9	10–12	—	—	Absent	Absent	Boulenger (1914)
C. minor	71	Absent	37–44	Subequal	8–12	11	7	—	—	Shallow	Banded	Oliver and Richards (2012)
C. murua	113	?	?	Enlarged	24–25	?	?	?	?	Absent	Banded	Rösler et al. (2007)
C. novaeguineae	158	Absent	35–59	Subequal	16–22	—	—	24–43	—	Absent	Banded	Rösler et al. (2007)
C. papuensis	70	Present	45–57	Subequal	20–24	11	Absent	—	Subequal	Pit	Blotched	This study
C. rex	172	Present	49–60	Enlarged	10–19	—	—	28–38	—	Absent	Banded	Oliver et al. (2016)
C. robustus	161	Absent	38–50	Subequal	25–32	—	—	75–85	—	Absent	Banded	Kraus (2008)
C. sermowaiensis	112	Present	44–48	Subequal	25–29	Absent	Absent	—	Subequal	Absent	Banded	Oliver et al. (2020)
C. serratus	139	Absent	?	Subequal	27	—	—	87	—	Absent	Banded	Kraus (2007)
C. tanim	97	Absent	46–54	Subequal	11–14	15–17	30–31	—	—	Absent	Banded	Nielsen and Oliver (2017)
C. tripartitus	148	Absent	47–55	Enlarged	26–31	—	—	64–78	—	Absent	Banded	Kraus (2008)
C. zugi	159	Absent	45–52	Enlarged	25–27	?	?	?	?	Absent	Blotched	Oliver et al. (2008)

FIG. 4.—(A) The holotype (MZB.Lace. 14052) of *Cyrtodactylus papeda* sp. nov. and (B) the habitat at Kawasi, Obi Island. Photographs by FHF. A color version of this figure is available online.

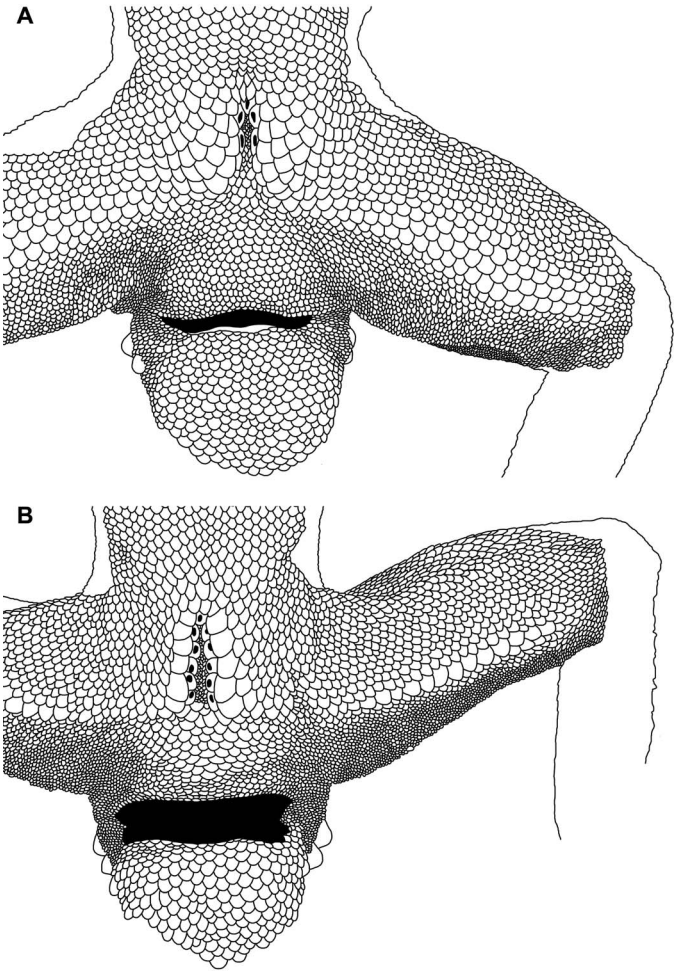

FIG. 5.—Precloacal depression posterior and enlarged femoral and precloacal scales of (A) *Cyrtodactylus papeda* sp. nov. holotype MZB.Lace. 14052 and (B) *C. papuensis* holotype ZMA.RENA 10937. Illustrations by AATA (not to scale).

smooth, subimbricate; digits well developed, inflected at basal interphalangeal joints, digits slightly narrower distal to inflection; subdigital lamellae transversely expanded along the entire length of each digit, but slightly compressed in both length and width immediately distal to interphalangeal inflection; 11 F_1, 16 F_2, 19 F_3, 18 F_4, and 17 F_5; claws well developed, sheathed by 2 dorsal scales and 1 ventral scale. Hindlimbs longer than forelimbs, TBL 17.6% of SVL; covered dorsally by granular scales interspersed with larger, conical tubercles; anterioroventral scales of thigh rounded, smooth, flat, subimbricate to juxtaposed, larger than dorsal scales; enlarged femoral and precloacal scales arranged in a continuous series, with the enlarged femoral scales arranged in 2 or 3 rows; femoral pores absent; males with 5 precloacal pore-bearing scales in deep groove, pores and groove absent in females; posterior-ventral scales of thigh very small extending, contrasting against enlarged femoral scales; ventral scales on tibia smooth, flat, subimbricate; plantar scales slightly raised; digits well developed, inflected at basal metapodial-phalangeal joints, digits slightly narrower distal to inflection; subdigital lamellae transversely expanded along the entire length of each digit, but slightly compressed in both length and width immediately distal to interphalangeal inflection; 12 T_1, 18 T_2, 21 T_3, 22 T_4, and 19 T_5; claws well developed, sheathed by 2 dorsal scales and 1 ventral scale.

Original tails slightly longer than body, TL 135.2% of SVL; segmented; dorsally with keeled tubercles anteriorly one-third of the original TL; tubercles arranged in transverse rows forming whorls; two postcloacal tubercles (spur) on each side in both sexes. Original subcaudal scales small, hexagonal, without enlarged transverse plates. Regenerated tails lack dorsal tubercles and have transversely enlarged subcaudals. The holotype is with a bifurcated tail.

Coloration.—After 5 yr in preservative, dorsum is light brown patterned with seven or eight irregular narrow transverse darker brown markings between axilla and groin; a further dark-brown stripe extends from the postnasal region past the eye and continues to the upper ear opening. Dorsal side of tail bended, on base the dark bands narrowed, widening as the tail tapers, 9 or 10 dark cross bands, the dark cross band extended to ventral forming whorl, tip always darks.

In life, same color as in preservative, but all the paler brown areas on the dorsum visible in a range of gray, cream, or brownish yellow; supercilium and canthus golden yellow.

Variation.—Adult males (MZB.Lace. 14575, 14576, 14578) reach 56.6–62.9 mm SVL and adult females (MZB.Lace. 14053, 14574, 14577) reach 55.9–84.0 mm; rostral bordered dorsally by 3 or 4 postrostral scales; 10–13 supralabial scales and 9 or 10 infralabial scales to angle of

Fig. 6.—An adult individual of *Cyrtodactylus papuensis* (not collected) from Papua New Guinea. Photograph by S.J. Richards. A color version of this figure is available online.

jaw; 14–17 dorsal tubercle rows; 27–34 paravertebral tubercles in each row; 45–54 ventral scale rows between ventrolateral body folds across the belly; subdigital lamellae on fingers, namely, 10–12 F_1, 14–17 F_2, 16–20 F_3, 18–21 F_4, and 16–18 F_5; and subdigital lamellae on toes, namely, 10–13 T_1, 16–18 T_2, 20–23 T_3, 21–23 T_4, and 19–20 T_5; 2 or 3 postcloacal tubercles (spur) on each side in both sexes.

Comparisons.—*Cyrtodactylus papeda* sp. nov. is most similar to *C. papuensis* (Figs. 5B and 6) but differs in having 14–17 dorsal tubercle rows (vs. 19–23), a deep groove-like precloacal depression with 5 pores (vs. narrow chevron-shaped depression with 11 pores) in males, enlarged femoral and precloacal scales in continuous series (vs. interrupted), and enlarged femoral scales arranged in multiple rows (vs. a single row). The new species differs from other congeners in the *C. marmoratus* group as follows: from *Cyrtodactylus semiadii* Riyanto, Bauer, and Yudha 2014 by being much larger (SVL 84.0 mm vs. 58.0 mm), by having preclocal pores in males (vs. absent), and by lacking femoral pores in males (vs. present); and from *C. marmoratus* by the presence of dorsal tubercles on brachium and forearm (vs. absent) and its smaller number of pores (5 precloacal pores vs. 43–57 precloacal and femoral pores in continuous series).

The new species differs from the three other *Cyrtodactylus* species in the northern Moluccas as follows: from *C. deveti* by its smaller maximum SVL of 84 mm (vs. 106 mm), absence of femoral pores (vs. present), presence of a precloacal grove (vs. absent), and median subcaudal scales subequal (vs. enlarged); from *C. halmahericus* by the absence of femoral pores (vs. present) and having 45–54 ventral scale rows across the belly (vs. 39–42); and from *C. nuaulu* in having enlarged femoral scales (vs. subequal), absence of whorls of enlarged dentate tubercles in tail (vs. present), and absence of a lateral groove at anterior section of the tail (vs. present).

We compared the new species to the recognized Wallacean species (Table 5). Further comparisons between the new species to the other recognized *Cyrtodactylus* in Melanesia are provided in Table 6.

Etymology.—The specific epithet is an invariable noun in apposition and refers to *papeda* (in Indonesian language), a traditional fiber-rich, cholesterol-low food in Moluccas and West Papua made from sago (*Metroxylon sagu*, family Arecaceae) starch. Here, we used this epithet to honor (promote) a traditional culinary feature of Obi Island and to showcase this new endemic gecko species to the public. *Papeda* is white in color, with the texture resembling sticky glue, and the cuisine is usually served with tuna fish and flavored with saffron. Suggested vernacular names are "cecak jarilengkung Obi" and Obi bent-toad gecko, in Bahasa Indonesia and English, respectively.

Natural history.—All individuals were collected from Kawasi, the west coastal area of Obi Island. The habitat was swampy vegetation of mangroves, screw pines, and a secondary forest associated with a scrubland. They were usually found at night, between 30 cm to 3 m above the ground and mostly on tree trunks. They were moderately common, with at least two or more individuals often observed on one tree. It was sympatric with *H. frenatus* and found from near sea level up to 200 m above sea level and is known to range at least 1-km inland from the coast. The presence of *H. frenatus* has been reported from this island by De Rooij (1915).

Discussion

Based on genetic data present in Grismer et al. (2021) and this study, we now consider that the *C. marmoratus* group includes at least four named species, as follows: two from Java (*C. marmoratus* and *C. semiadii*); one from Melanesia (*C. papuensis*); and one from Wallacea (*C. papeda* sp. nov.). Additional candidate species in this group are also known from Java and Sumatra (O'Connell et al. 2019). The *C. marmoratus* group is one of three *Cyrtodactylus* lineages that have crossed into Wallacea and Melanesia (with others being the *C. darmandvillei* group and the ancestor of the main Melanesian radiation of *Cyrtodactylus*). All four members of the *C. marmoratus* group share nonenlarged subcaudals and are also relatively small *Cyrtodactylus* (<85 mm). The description of *C. papeda* sp. nov. from Obi Island (Fig. 1) fills a geographic gap in the previously documented distribution of the *C. marmoratus* group.

Many *Cyrtodactylus* species from Wallacea and Melanesia have no genetic evidence to define their phylogenetic relationships. However, based on distribution and morphology, Grismer et al. (2021) assigned the following six species to two respective species-groups: *Cyrtodactylus aaroni* and *Cyrtodactylus irianjayaensis* into the *Cyrtodactylus novaeguineae* group and *Cyrtodactylus celatus*, *Cyrtodactylus tambora*, *Cyrtodactylus tanahjampea*, and *Cyrtodactylus wetarensis* into the *C. darmandvillei* group. Amarasinghe et al. (2020) assigned *Cyrtodactylus jatnai* into the *C. darmandvillei* group based on morphology, and genetic data for this species also confirm this placement (Oliver et al. 2018; Grismer et al. 2021). Morphological characters also suggest *C. deveti* is likely allied to taxa in the Melanesian radiation of *Cyrtodactylus* rather than other species in the Moluccas (Grismer et al. 2021). *Cyrtodactylus spinosus* is considered an orphaned species due to its unique stand-alone placement in molecular phylogenetic analyses (Grismer et al. 2021).

The phylogenetic positions of most of nine additional Wallacean species have not been commented on. Based on our observations, here, we tentatively assign *Cyrtodactylus hitchi* to the *C. darmandvillei* group due to the quite prominent and densely arranged enlarged tubercles across the body. *Cyrtodactylus batik* is a morphologically unique species with enlarged subcaudals. Phylogenetic data are required to assign the remaining Wallacean species to species-groups, namely, *Cyrtodactylus fumosus*, *Cyrtodactylus gordongekkoi*, *C. halmahericus*, *Cyrtodactylus laevigatus*, *C. nuaulu*, *Cyrtodactylus tahuna*, and *Cyrtodactylus wallacei*.

The lack of genetic data and poor understanding of the phylogenetic affinities of most Wallacean *Cyrtodactylus* highlight our incomplete knowledge of the herpetofauna of this region. Obi is especially poorly known, with studies limited to work on *Varanus* monitors (Koch and Böhme 2010; Weijola 2010). The discovery of a genetically and morphologically distinct new *Cyrtodactylus* suggests additional unrecognized lizard taxa await discovery and description on Obi and on other Islands of the Moluccas.

Acknowledgments.—AR, AH, MM, and YSF thank the Indonesian Institute of Sciences via "KSK–Konstruksi Referensi Sekuen DNA Barcode dan Kajian Genetika Populasi untuk Keperluan Konservasi," CITES, "Forensik dan Pengembangan Bank DNA Fauna Indonesia," and "KSK–Penguatan Kelembagaan dalam Melaksanakan Mandat Sebagai Otoritas Keilmuan Terkait Keanekaragaman Hayati" for support in laboratory work. FHF thanks Harita Group Obi Site and biodiversity monitoring survey team for facilitating surveys in 2017–2018 and 2020–2021. AATA thanks E. Dondorp (RMNH, the Netherlands), P.D. Campbell (NHMUK, UK), and E. Stöckli (NMB, Switzerland) for facilitating the in-house study and/or for measurements/pictures of specimens under their care; J.A. McGuire is acknowledged for valuable comments and J. Supriatna and the staff of the Research Center for Climate Change, University of Indonesia for their support.

Literature Cited

Amarasinghe, A.A.T., M.B. Harvey, A. Riyanto and E.N. Smith. 2015. A new species of *Cnemaspis* (Reptilia: Gekkonidae) from Sumatra, Indonesia. Herpetologica 71:160–167.

Amarasinghe, A.A.T., A. Riyanto, M. Mumpuni and L.L. Grismer. 2020. A new bent-toed gecko species of the genus *Cyrtodactylus* Gray, 1827 (Squamata: Gekkonidae) from The West Bali National Park, Bali, Indonesia. Taprobanica 9:59–70.

Bauer, A.M., T.R. Jackman, E. Greenbaum, A. de Silva, V.B. Giri and I. Das. 2010. Molecular evidence for the taxonomic status of *Hemidactylus brookii* group taxa (Squamata: Gekkonidae). Herpetological Journal 20:129–138.

Boulenger, G.A. 1914. An annotated list of the batrachians and reptiles collected by the British Ornithologists' Union Expedition and the Wollaston Expedition in Dutch New Guinea. Transactions of the Zoological Society of London 20:247–275.

Brennan, I.G., A.M. Bauer, N.V. Tri, Y.Y. Wang, W.Z. Wang, Y.P. Zhang and R.W. Murphy. 2017. Barcoding utility in a mega-diverse, cross-continental genus: Keeping pace with *Cyrtodactylus* geckos. Scientific Reports 7:5592.

Brongersma, L.D. 1934. Contributions to Indo-Australian herpetology. Zoologische Mededelingen 17:161–251.

Brongersma, L.D. 1948. Lizards from the island of Morotai (Moluccas). Proceedings van de Koninklijke Nederlandse Akademie van Wetenschappen Section C 51:486–495.

Brown, W.C., and F. Parker. 1973. A new species of Cyrtodactylus (Gekkonidae) from New Guinea with a key to species from the island. Breviora 417:1–7.

De Rooij, N. 1915. The Reptiles of the Indo-Australian Archipelago. I. Lacertilia, Chelonia, Emydosauria. E.J. Brill, the Netherlands.

Edgar, P., and R. Lilley. 1993. Herpetofauna survey of Manusela National Park. Pp. 131–141 in Natural History of Seram (I.D. Edwards, A.A. McDonald and J. Proctor, eds.). Intercept Ltd., UK.

Gill, F., and D. Donsker (eds.).2012. IOC World Bird Names, Version 11.2. Available at http://www.worldbirdnames.org. Accessed on 2 September 2021. International Ornithologists' Union, USA.

Gray, J.E. 1831. A synopsis of the species of Class Reptilia. Pp. 1–110 in The Animal Kingdom Arranged in Conformity with its Organization by the Baron Cuvier with Additional Descriptions of all the Species Hither Named, and of Many Before Noticed (E. Griffith and E. Pidgeon, eds.). Whittaker, Treacher and Co., UK.

Grismer, L.L., P.L. Wood, Jr., N.A. Poyarkov, … J.L. Grismer. 2121. Phylogenetic partitioning of the third-largest vertebrate genus in the world, *Cyrtodactylus* Gray, 1827 (Reptilia; Squamata; Gekkonidae) and its relevance to taxonomy and conservation. Vertebrate Zoology 71:101–154.

Günther, R., and H. Rösler. 2003. Eine neue Art der Gattung *Cyrtodactylus* Gray, 1827 aus dem Westen von Neuguinea (Reptilia: Sauria: Gekkonidae). Salamandra 38:195–212.

Harvey, M.B., K.A. O'Connell, G. Barraza, A. Riyanto, N. Kurniawan and E.N. Smith. 2015. Two new species of *Cyrtodactylus* (Squamata: Gekkonidae) from the Southern Bukit Barisan Range of Sumatra and an estimation of their phylogeny Zootaxa 4020:495–516.

Hoang, D.T., O. Chernomor, A. von Haeseler, M.B. Quang and L. Sy Vinh. 2017. Supplementary data: Ufboot 2: Improving the ultrafast bootstrap approximation. Molecular Biology and Evolution 35:518–522.

Johnson, C.B., S.H.E. Quah, S. Anuar, … L.L. Grismer. 2012. Phylogeography, geographic variation, and taxonomy of the bent-toed gecko *Cyrtodactylus quadrivirgatus* Taylor, 1962 from Peninsular Malaysia with the description of a new swamp dwelling species. Zootaxa 3406:39–58.

Karin, B.P., A.L. Stubbs, U. Arifin, … J.A. Mcguire. 2018. The herpetofauna of the Kei Islands (Maluku, Indonesia): Comprehensive report on new and historical collections, biogeographic patterns, conservation concerns, and an annotated checklist of species from Kei Kecil, Kei Besar, Tam, and Kur. Raffles Bulletin of Zoology 66:704–738.

Kathriner, A., A.M. Bauer, M. O'Shea, C. Sanchez and H. Kaiser. 2014. Hiding in plain sight: A new species of bent-toed gecko (Squamata: Gekkonidae: *Cyrtodactylus*) from West Timor, collected by Malcolm Smith in 1924. Zootaxa 3900:555–568.

Koch, A., and W. Böhme. 2010. Heading east: A new subspecies of *Varanus salvator* from Obi Island, Maluku province, Indonesia with a discussion about easternmost natural occurrence of Southeast Asia water monitor lizards. Russian Journal of Herpetology 17:299–309.

Kraus, F. 2007. A new species of *Cyrtodactylus* (Squamata: Gekkonidae) from western Papua New Guinea. Zootaxa 1425:63–68.

Kraus, F. 2008. Taxonomic partitioning of *Cyrtodactylus louisiadensis* (Lacertilia: Gekkonidae) from Papua New Guinea. Zootaxa 1883:1–27.

Kraus, F., and V. Weijola. 2019. New species of *Cyrtodactylus* (Squamata: Gekkonidae) from Karkar Island, Papua New Guinea. Zootaxa 4695:529–540.

Kumar, S., G. Stecher, M. Li, C. Knyaz and K. Tamura. 2018. MEGA X: Molecular evolutionary genetics analysis across computing platforms. Molecular Biology and Evolution 35:1547–1549.

Lanfear, R., B. Calcott, S.Y. Ho and S. Guindon. 2012. PartitionFinder: Comined selection of partitioning schemes and substitution models for phylogenetic analyses. Molecular Biology and Evolution 29:1695–1701.

Linkem, C.W., J.A. McGuire, C.J. Hayden, M.I. Setiadi, D.P. Bickford and R.M. Brown. 2008. A new species of bent-toed gecko (Gekkonidae: *Cyrtodactylus*) from Sulawesi Island, eastern Indonesia. Herpetologica 64:224–234.

Mecke, S., L. Hartmann, F. Mader, M. Kieckbusch and H. Kaiser. 2016a. Redescription of *Cyrtodactylus fumosus* (Müller, 1895) (Reptilia: Squamata: Gekkonidae), with a revised identification key to the bent-toed geckos of Sulawesi. Acta Herpetologica 11:151–160.

Mecke, S., M. Kieckbusch, L. Hartmann and H. Kaiser. 2016b. Historical considerations and comments on the type series of *Cyrtodactylus marmoratus* Gray, 1831, with an updated comparative table for the bent-toed geckos of the Sunda Islands and Sulawesi. Zootaxa 4175:353–365.

Mertens, R. 1929. Zwei neue Haftzeher aus dem Indo-Australischen Archipel (Reptiles). Senckenbergiana 11:237–241.

Minh, B.Q., M.A.T. Nguyen and A. von Haeseler. 2013. Ultrafast approximation for phylogenetic bootstrap. Molecular Biology and Evolution 30:1188–1195.

Nielsen, S.V., and P.M. Oliver. 2017. Morphological and genetic evidence for a new karst specialist lizard from New Guinea (*Cyrtodactylus*: Gekkonidae). Royal Society Open Science 4:170781.

O'Connell, K.A., U. Smart, I. Sidik, A. Riyanto, N. Kurniawn and E.N. Smith.

2019. Diversification of bent-toed geckos (*Cyrtodactylus*) on Sumatra and West Java. Molecular Phylogenetics and Evolution 134:1–11.
Oliver, P.M., and S.J. Richards. 2012. A new species of small bent-toed gecko (*Cyrtodactylus*: Gekkonidae) from the Huon Peninsula, Papua New Guinea. Journal of Herpetology 46:488–493.
Oliver, P.M, B. Tjaturadi, M. Mumpuni, K. Krey and S.J. Richards. 2008. A new species of large *Cyrtodactylus* (Squamata: Gekkonidae) from Melanesia. Zootaxa 1894:59–68.
Oliver, P.M., P. Edgar, M. Mumpuni, D.T. Iskandar and R. Lilley. 2009. A new species of bent-toed gecko (*Cyrtodactylus*: Gekkonidae) from Seram Island, Indonesia. Zootaxa 2115:47–55.
Oliver, P.M., K. Krey, M. Mumpuni and S.J. Richards. 2011. A new species of bent-toed gecko (*Cyrtodactylus*, Gekkonidae) from the North Papuan Mountains. Zootaxa 2930:22–32.
Oliver, P.M., S.J. Richards and M. M.Sistrom, 2012. Phylogeny and systematics of Melanesia's most diverse gecko lineage (*Cyrtodactylus*, Gekkonidae, Squamata). Zoologica Scripta 41:437–454.
Oliver, P.M., S.J. Richards, M. Mumpuni and H. Rösler. 2016. The Knight and the King: Two new species of giant bent-toed gecko (*Cyrtodactylus*, Gekkonidae, Squamata) from northern New Guinea, with comments on endemism in the North Papuan Mountains. ZooKeys 562:105–130.
Oliver, P.M., M.P.K. Blom, H.G. Cogger, R.N. Fisher, J.Q. Richmond and J.C.Z. Woinarski. 2018. Insular biogeographic origins and high phylogenetic distinctiveness for a recently depleted lizard fauna from Christmas Island, Australia. Biology Letters 14:20170696.
Oliver, P.M., D.T. Karkkainen, H. Rösler and S.J. Richards. 2019. A new species of *Cyrtodactylus* (Squamata: Gekkonidae) from central New Guinea. Zootaxa 4671:119–128.
Oliver, P.M., R. Hartman, C.D. Turner, T.A. Wilde, C.C. Austin and S.J. Richards. 2020. A new species of *Cyrtodactylus* Gray (Gekkonidae: Squamata) from Manus Island, and extended description and range extension for *Cyrtodactylus sermowaiensis* (De Rooij). Zootaxa 4728:341–356.
R Core Team. 2021. R: A language and environment for statistical computing, Version 4.0.4. Available at https://www.R-project.org/. R Foundation for Statistical Computing, Austria.
Riyanto, A. 2012. *Cyrtodactylus hikidai* sp. nov. (Squamata: Gekkonidae): A new bent toed gecko from Mount Ranai, Bunguran Island, Indonesia. Zootaxa 3583:22–30.
Riyanto, A., A.M. Bauer and D.N. Yudha. 2014. A new small karst-dwelling species of *Cyrtodactylus* (Reptilia: Squamata: Gekkonidae) from Java, Indonesia. Zootaxa 3785:589–599.
Riyanto, A., L.L. Grismer and P.L. Wood, Jr. 2015. *Cyrtodactylus rosichonariefi* sp. nov. (Squamata: Gekkonidae), a new swamp-dwelling bent-toed gecko from Bunguran Island (Great Natuna), Indonesia. Zootaxa 3964:114–124.
Riyanto, A., H. Kurniati and A. Engilis. 2016. A new bent-toed gecko (Squamata: Gekkonidae) from the Mekongga Mountains, Southeast Sulawesi, Indonesia. Zootaxa 4109:59–72.
Riyanto, A., Mulyadi, J.A. McGuire, M.D. I.H. Kusrini, Febylasmia, Basyir and H. Kaiser. 2017. A new small bent-toed gecko of the genus *Cyrtodactylus* (Squamata: Gekkonidae) from the lower slopes of Mount Tambora, Sumbawa Island, Indonesia. Zootaxa 4242:517–528.
Riyanto, A., E. Arida and A. Koch. 2018a. *Cyrtodactylus tahuna* sp. nov., a new bent-toed gecko (Reptilia: Squamata: Gekkonidae) from Sangihe Island, North Sulawesi, Indonesia. Zootaxa 4399:220–232.
Riyanto, A., A. Hamidy and J.A. McGuire. 2018b. A new bent-toed gecko (*Cyrtodactylus*: Squamata: Gekkonidae) from the Island of Tanahjampea, South Sulawesi, Indonesia. Zootaxa 4442:122–136.
Riyanto, A., A. Farajallah, A. Hamidy, Y.S. Fitriana, M. Munir, N. Kurniawan and E.N. Smith. 2020. Taxonomic evaluation of two similar bent-toed geckos (Squamata: Gekkonidae: *Cyrtodactylus* Gray, 1827) from East Java, Indonesia. Zootaxa 4830:186–196.
Ronquist, F., and J.P. Huelsenbeck. 2003. MrBayes 3: Bayesian phylogenetic inference under mix models. Bioinformatics 19:1572–1574.
Rösler, H., S.J. Richards and R. Günther. 2007. Remarks on morphology and taxonomy of geckos of the genus *Cyrtodactylus* Gray, 1827, occurring east of Wallacea, with descriptions of two new species (Reptilia: Sauria: Gekkonidae). Salamandara 43:193–230.
Sambrook, J., E.F. Fritschi and T. Maniatis. 1989. Molecular Cloning: A Laboratory Manual, 2nd edition. Cold Spring Harbor Laboratory Press, USA.
Tallowin, O.J.S., K. Tamar, S. Meiri, A. Allison, F. Kraus, S.J. Richards and P.M. Oliver. 2018. Early insularity and subsequent mountain uplift were complementary drivers of diversification in a Melanesian lizard radiation (Gekkonidae: *Cyrtodactylus*). Molecular Phylogenetics and Evolution 125:29–39.
Uetz, P., and J. Hallermann. 2021. The reptile database. Available at http://www.reptile-database.org. Accessed on 20 December 2021.
Uetz, P., S. Cherikh, G. Shea, ... V. Wallach. 2019. A global catalog of primary reptile type specimens. Zootaxa 4695:438–450.
van Welzen, P.C., J.A.N. Parnell and J.W.F. Slik. 2011. Wallace's Line and plant distributions: Two or three phytogeographical areas and where to group Java? Biological Journal of the Linnean Society 103:531–545.
Weijola, V. 2010. Geographical distribution and habitat use of monitor lizards of the North Moluccas. Biawak 4:7–23.
Wood, P.L., Jr., M.P. Heinicke, T.R. Jackman and A.M. Bauer. 2012. Phylogeny of bent-toed geckos (*Cyrtodactylus*) reveals a west to east pattern of diversification. Molecular Phylogenetics and Evolution 65:992–1003.
Zar, J.H. 2010. Biostatistical Analysis, 5th edition. Prentice Hall Inc., USA.

Accepted on 23 December 2021
ZooBank.org registration LSID: E6B72F33-FA4B-4407-B67C-767BD4C3802F
Published on 1 March 2022
Associate Editor: Bryan Stuart

APPENDIX

Other Specimens Examined

Cyrtodactylus batik.—Indonesia: Central Sulawesi: MZB.Lace. 8511 (holotype).

Cyrtodactylus celatus.—Indonesia: Timor: TBMNH 1926.10.30.45 (holotype), ZSM 556/2002.

Cyrtodactylus darmandvillei.—Indonesia: Flores: ZMA.RENA 10943–44 (syntypes); Timor: FMNH 154845.

Cyrtodactylus deveti.—Indonesia: Halmahera: MZB.Lace. 7956, 8164–65; Morotai Island: RMNH 2775 (holotype), 8683 (paratype).

Cyrtodactylus fumosus.—Indonesia: North Sulawesi: NMB 2662 (holotype).

Cyrtodactylus gordongekkoi.—Indonesia: Lombok: ZRC 2.3381 (paratype).

Cyrtodactylus halmahericus.—Indonesia: Halmahera: MZB.Lace. 6087, 13250.

Cyrtodactylus hitchi.—Indonesia: Southeast Sulawesi: MZB.Lace. 8642 (holotype), 8635–40 (paratypes), 8646 (paratype), 8648 (paratype).

Cyrtodactylus jatnai.—Indonesia: Bali: UIMZ 0085 (holotype), UIMZ 0082–84 (paratypes), 0101–102 (paratypes), MZB.Lace. 8725–37 (paratypes).

Cyrtodactylus jellesmae.—Indonesia: Central Sulawesi: NMB 2660 (lectotype); South Sulawesi: MZB.Lace. 5686, 5688; North Sulawesi: NMB 2661 (paralectotype); MZB.Lace. 6943.

Cyrtodactylus laevigatus.—Indonesia: Komodo: MZB.Lace. 979.

Cyrtodactylus nuaulu.—Indonesia: Seram: MZB.Lace. 2326 (holotype), 2325, 2327–28, UIMZ 0181.

Cyrtodactylus papuensis.—Southern New Guinea: ZMA.RENA 10937 (holotype); Indonesia: West Papua: MZB.Lace. 12115, 14969–70, 15160–66.

Cyrtodactylus spinosus.—Indonesia: Central Sulawesi: MZB.Lace. 7024 (holotype), 7025–29 (paratypes).

Cyrtodactylus tahuna.—Indonesia: Sangihe Island, North Sulawesi: MZB.Lace. 5123 (holotype), 5097, 5133 (paratypes).

Cyrtodactylus tambora.—Indonesia: Sumbawa: MZB.Lace. 3298 (holotype), 13297, 13909 (holotypes).

Cyrtodactylus tanahjampea.—Indonesia: Tanahjampea Island, South Sulawesi: MZB.Lace. 5675 (holotype), 5671–72 (paratypes), 5674 (paratype).

Cyrtodactylus wallacei.—Indonesia: Kabaena Island, Southeast Sulawesi: MZB.Lace. 4264 (paratype).

Cyrtodactylus zugi.—Indonesia: Raja Ampat Archipelago (West Papua): MZB.Lace. 5574 (holotype), 5573 (paratype), 5575 (paratype).